Post-Newtonian Sachs-Wolfe effect

Eric V. Linder

Imperial College, Prince Consort Road, London SW7 2BZ, UK (el@ic.ac.uk)

Abstract. Deviations from the Friedmann-Robertson-Walker (FRW) cosmological model in the form of density inhomogeneities induce observational effects on the light propagating through these fluctuations. Using a rigorously parametrized metric whose pseudo-Newtonian potential is related to (possibly nonlinear) density inhomogeneities through a relativistic Green function, the behavior of radiation propagating through this approximation to our universe is investigated, without relying on any spatial averaging or late time, short perturbation wavelength Newtonian limit. In certain regimes the energy shift of a photon due to density fluctuations, the Sachs-Wolfe effect, is found to deviate significantly from the linearized relativity (Poisson-Newton) result, but the corresponding cosmic microwave background temperature fluctuations are still below 10^{-6} on small scales. On large scales this can be treated as an effective transfer function for the density power spectrum, altering the scaling of the amplitudes of large versus small scale power.

Key words: relativity – gravitation – cosmic microwave background

1. Introduction

A self consistent treatment of observations in a realistically inhomogeneous universe involves relativistic cosmological calculation of both the influence of the inhomogeneity on the metric and the metric on the light. Often both are treated only within the late time, short wavelength Newtonian approximation where the density determines a spatial metric fluctuation by the Poisson equation and the metric influences the propagation through an essentially local impulse. Here we use recent improvements beyond "Newtonian" order to investigate relativistically light propagation, especially from the last scattering surface of the cosmic microwave background radiation (CMB).

In Sect. 2 we use a relativistically rigorous metric (Futamase 1989) describing a universe deviating by gravitational potential perturbations from FRW, accurate to a well defined order, to obtain the Einstein field equations. The Green function solution of Jacobs, Linder, & Wagoner (1992=JLW1; 1993=JLW2) relates the gravitational potential to the density inhomogeneity for arbitrary density contrasts, i.e. without restrictions to the linear regime. We identify those regions in parameter space where

post-Newtonian effects are appreciable, as well as deriving analytic expressions for the derivatives of the potential, useful in light propagation calculations. In Sect. 3 we concentrate on the Sachs-Wolfe effect, where density inhomogeneities generate temperature anisotropies in the CMB, evaluating the deviation of the Green function results from the standard Newtonian ones. The results are given both numerically and by analytic order of magnitude arguments to reveal where the deviations arise. In addition we find an effective correction to the density power spectrum P_k which alters the intrinsic scaling of its amplitude from small to large scales.

While the redshift of light propagating through inhomogeneities is well studied (see, e.g., Ma & Bertschinger 1995 for the Sachs-Wolfe effect in linear perturbation theory and Seljak 1996 for the Rees-Sciama effect in numerical simulations), it has been considered within linearized general relativity and not the post-Newtonian formalism of Futamase 1989, JLW1, and JLW2. That possibly significant differences may arise can be seen from the diffusion equation analogy of JLW2 as well as the relativistic approaches of Kodama & Sasaki 1984 and Futamase & Schutz 1983, which agree with the results here that there exist corrections to the linearized general relativistic solution – the Poisson-Newton equation between the gravitational potential perturbation appearing in the metric, ϕ, and the density fluctuation $\delta\rho$. That is just the late time, short wavelength "Newtonian" approximation.

2. Gravitational potential

Under the assumptions that the gravitational potential fluctuations ϕ are small, parametrized by $\epsilon^2 \ll 1$, and their peculiar accelerations $\nabla\phi \sim \epsilon^2/\kappa$ are small (thus ensuring that peculiar motions remain much less than the speed of light) for characteristic inhomogeneity scales $l = \kappa L$ with L the background curvature or horizon length scale, the following metric provides a consistent description:

$$ds^2 = a^2(\eta)\left[-(1+2\phi)d\eta^2 + (1-2\phi)\gamma_{ij}dx^i dx^j\right] \tag{1}$$

(Futamase 1989; JLW1). Here a is the FRW expansion factor (to the order required), η the conformal time, and γ_{ij} the spatial part of the conformally stationary Robertson-Walker metric. The conditions are expected to hold cosmologically everywhere

far outside the radii of black holes and neutron stars. We call the full time dependence and presence of ϕ in the spatial part of the metric the post-Newtonian corrections.

The Einstein field equations produce the following relation between the scalar harmonic modes of ϕ and the density contrast $\Delta = \delta\rho/\bar{\rho}$,

$$3\frac{\dot{a}}{a}\dot{\phi}(\eta, \boldsymbol{q}) + (q^2 + 8\pi a^2\bar{\rho} - 6k)\,\phi(\eta, \boldsymbol{q}) = -4\pi a^2\bar{\rho}\Delta(\eta, \boldsymbol{q}), \quad (2)$$

(JLW1; JLW2). Here k is the trichotomic FRW curvature parameter, $\bar{\rho}$ the unperturbed density, and $\boldsymbol{q}$ is the mode variable conjugate to position. No restrictions are made on the size of Δ, i.e. the density field could be nonlinear.

Solution of this equation gives (JLW2)

$$\phi(\eta, \boldsymbol{x}) =$$

$$-(4\pi/3)\int_{\eta_0}^{\eta} du\,(a^3\bar{\rho}/\dot{a})\int d^3\boldsymbol{y}\,G(u, \eta, \boldsymbol{x}, \boldsymbol{y})\,\Delta(u, \boldsymbol{y})$$

$$+\int d^3\boldsymbol{y}\,G(\eta_0, \eta, \boldsymbol{x}, \boldsymbol{y})\,\phi(\eta_0, \boldsymbol{y}), \quad (3)$$

with the Green function in the $k = 0$ case (used here throughout)

$$G(u, \eta, \boldsymbol{x}, \boldsymbol{y}) =$$

$$[a(u)/a(\eta)]\,[4\pi C(u, \eta)]^{-3/2}\exp\{-|\boldsymbol{x} - \boldsymbol{y}|^2/4C(u, \eta)\}$$

$$C(u, \eta) = (1/3)\int_u^{\eta} dw\,(a/\dot{a}). \quad (4)$$

Transformation of the time integration variable to $E = |\boldsymbol{x} - \boldsymbol{y}|/2C^{1/2}(u, \eta)$ reveals

$$\phi(\eta, \boldsymbol{x}) = -(2/\sqrt{\pi})$$

$$\int d^3\boldsymbol{y}\,a^{-1}(\eta)|\boldsymbol{x} - \boldsymbol{y}|^{-1}\int_{E_0}^{\infty} dE\,[a^3\bar{\rho}\Delta(E, \boldsymbol{y})]\,e^{-E^2}, \quad (5)$$

where $E_0 = |\boldsymbol{x} - \boldsymbol{y}|/2C^{1/2}(\eta_0, \eta)$.

In the Newtonian limit of late times ($\eta \gg \eta_0$) and subhorizon scales ($\kappa \ll 1$), $E_0 \to 0$ and it is found that

$$\phi(\eta, \boldsymbol{x}) = -\int d^3\boldsymbol{y}\,a^3\frac{\bar{\rho}\Delta(\eta, \boldsymbol{y})}{a|\boldsymbol{x} - \boldsymbol{y}|} \quad (6)$$

(JLW2), the usual result. [We have neglected the second, initial conditions term from (3) due to its exponential die off far from the initial hypersurface, but see Sect. 3.3.]

Going beyond JLW2 we adopt a dust background ($a = a_0\eta^2 = 2H_0^{-1}\eta^2$ where H_0 is the Hubble constant) and inhomogeneity behavior $\Delta(u, \boldsymbol{y}) = f(\boldsymbol{y})\bar{\rho}^{-1}\,[a(u)/a_0]^{-3+p}$ to yield

$$\phi(\eta, \boldsymbol{x}) = -\frac{2}{a_0\sqrt{\pi}}\left[\frac{a(\eta)}{a_0}\right]^{p-1}$$

$$\int d^3\boldsymbol{y}\,\frac{f(\boldsymbol{y})}{|\boldsymbol{x} - \boldsymbol{y}|}\int_{E_0}^{\infty} dE\,\left[1 - 3\frac{|\boldsymbol{x} - \boldsymbol{y}|^2}{\eta^2}E^{-2}\right]^p e^{-E^2}. \quad (7)$$

In the Newtonian limit this reduces to $\phi(\eta, \boldsymbol{x}) = -a_0^{-1}[a(\eta)/a_0]^{p-1}\int d^3\boldsymbol{y}\,f(\boldsymbol{y})/|\boldsymbol{x} - \boldsymbol{y}|$. Some particular cases of interest are $p = 0$ (density unevolving in physical coordinates) and $p = 1$ (as for the growth of linear density fluctuations $\Delta \ll 1$):

$$\phi(\eta, \boldsymbol{x})_{p=0} = -\frac{1}{a(\eta)}\int d^3\boldsymbol{y}\,\frac{f(\boldsymbol{y})}{|\boldsymbol{x} - \boldsymbol{y}|}\,\mathrm{erfc}(E_0) \quad (8a)$$

$$\phi(\eta, \boldsymbol{x})_{p=1} = -\frac{1}{a_0}\int d^3\boldsymbol{y}\,\frac{f(\boldsymbol{y})}{|\boldsymbol{x} - \boldsymbol{y}|}$$

$$\left\{\mathrm{erfc}(E_0)\left[1 + 6\frac{|\boldsymbol{x} - \boldsymbol{y}|^2}{\eta^2}\right] - \frac{2}{\sqrt{\pi}}\left(1 - \frac{\eta_0^2}{\eta^2}\right)E_0e^{-E_0^2}\right\} \quad (8b)$$

with erfc the complementary error function.

Since the geodesic equations determining light propagation involve derivatives of the potential we calculate in comoving coordinates $\nabla\phi$ and $\nabla_i\nabla_j\phi$.

$$\nabla\phi = -\frac{2}{a_0\sqrt{\pi}}\left[\frac{a(\eta)}{a_0}\right]^{p-1}\int d^3\boldsymbol{y}\,f(\boldsymbol{y})\frac{\boldsymbol{x} - \boldsymbol{y}}{|\boldsymbol{x} - \boldsymbol{y}|^3}\,I$$

$$I = \int_{E_0}^{\infty} dE\,U^p e^{-E^2}$$

$$+ 6p\frac{|\boldsymbol{x} - \boldsymbol{y}|^2}{\eta^2}\int_{E_0}^{\infty} dE\,U^{p-1}E^{-2}e^{-E^2} + U_0^p E_0 e^{-E_0^2}$$

$$U = 1 - 3\frac{|\boldsymbol{x} - \boldsymbol{y}|^2}{\eta^2}E^{-2}, \quad (9)$$

with special cases

$$\nabla\phi_{p=0} = \frac{1}{a(\eta)}\int d^3\boldsymbol{y}\,f(\boldsymbol{y})\frac{\boldsymbol{x} - \boldsymbol{y}}{|\boldsymbol{x} - \boldsymbol{y}|^3}$$

$$\left[\mathrm{erfc}(E_0) + \frac{2}{\sqrt{\pi}}E_0e^{-E_0^2}\right] \quad (10a)$$

$$\nabla\phi_{p=1} = \frac{1}{a_0}\int d^3\boldsymbol{y}\,f(\boldsymbol{y})\frac{\boldsymbol{x} - \boldsymbol{y}}{|\boldsymbol{x} - \boldsymbol{y}|^3}$$

$$\left[\left(1 - 6\frac{|\boldsymbol{x} - \boldsymbol{y}|^2}{\eta^2}\right)\mathrm{erfc}(E_0) + \frac{2}{\sqrt{\pi}}E_0e^{-E_0^2}\right]. \quad (10b)$$

The tidal field is $\nabla_i\nabla_j\phi$, necessary for calculations involving shear of a light ray bundle and the resulting image distortions. Because of its length we do not show the expression for it here but it is interesting to consider the Laplacian $\nabla^2\phi$. For $p = 0$

$$\nabla^2\phi = 4\pi a^{-1}\left\{f(\boldsymbol{x}) - \pi^{-3/2}\int d^3\boldsymbol{y}\,\frac{f(\boldsymbol{y})}{|\boldsymbol{x} - \boldsymbol{y}|^3}E_0^3 e^{-E_0^2}\right\}$$

$$= 4\pi a^{-1}\left\{f(\boldsymbol{x}) - (4\pi C_0)^{-3/2}\int d^3\boldsymbol{y}\,f(\boldsymbol{y})\,e^{-|\boldsymbol{x} - \boldsymbol{y}|^2/4C_0}\right\}, \quad (11)$$

where $C_0 = C(\eta_0, \eta)$.

The second term thus illustrates the (not linearized) general relativistic correction to the Poisson equation (in the fully specified longitudinal gauge), involving a gaussian weighting over the extent of the inhomogeneity. In the "Newtonian" limit the fluctuation is restricted to regions much smaller than the dispersion $(2C_0)^{1/2}$ so its contrast is averaged to zero, leaving the Poisson result, while in the opposite ("superhorizon" fluctuation) limit the gaussian becomes a delta function, giving the Laplace equation appropriate for a uniform density field.

3. Sachs-Wolfe effect

Given the metric (1) and the results (7), (9), (11) one can investigate light propagation behavior by writing down the geodesic equation, geodesic deviation, and the beam or Raychaudhuri equation. Properties of the photon bundle, such as convergence and shear, and applications of the geodesic deviation equation to astrophysical problems such as correlations of observables in terms of the density power spectrum are in ongoing research. Here we concentrate on the geodesic equation for individual photon four momentum, in particular the Sachs-Wolfe effect on the redshift.

In longitudinal gauge ($g_{0i} = 0$ and g_{ij} proportional to γ_{ij}; see Bardeen 1980 and Kodama & Sasaki 1984 for gauges and gauge invariance) the expression for the frequency of a photon emitted at η_e becomes

$$k^0(\eta) = k^0(\eta_e) \left[a(\eta_e)/a(\eta)\right] \left(1 - 2 \int_{\eta_e}^{\eta} du\, \hat{n} \cdot \boldsymbol{\nabla} \phi\right). \qquad (12)$$

(Note the more familiar time derivative of ϕ occurs in the unfully specified synchronous gauge expression, although one could convert the gradient into a time derivative and a surface term.) The ratio of expansion factors is the background cosmological redshift and $\hat{n}$ is the photon propagation unit vector. The inhomogeneity induced redshift, i.e. the Sachs-Wolfe effect, is then

$$z = 2 \int_{\eta_e}^{1} d\eta\, \hat{n} \cdot \boldsymbol{\nabla} \phi. \qquad (13)$$

Upon adopting a density field $\Delta(u, \boldsymbol{y})$ one can compute the gravitational potential gradient by (9) and hence obtain the redshift, or equivalently temperature anisotropy in the CMB. This, being an observable, is gauge independent. We consider compact density distributions, both static and time dependent, and then a field of inhomogeneities, along with the Fourier representation.

4. Static point mass

To derive analytic estimates of the dependence of the redshift on density parameters we begin by adopting the model of a simple point inhomogeneity of mass m at comoving position $\boldsymbol{y} = (y \cos\theta, y \sin\theta, 0)$. The x-axis is aligned with the light ray (perturbations to the photon path produce effects of smaller

Table 1. Point mass Sachs-Wolfe effect

	$(z/mH_0)_{N/PN}$		
$\Delta \sim a^0$	$\theta = 1''$	$\theta = 10''$	$\theta = 100''$
$z_m = 1$	218/134	192/108	166/82
$z_m = 3$	527/348	453/275	380/201
$\Delta \sim a$			
$z_m = 1$		1.93/-1.51	
$z_m = 3$		-0.14/-3.64	

order than we consider) and $y = 1 - (1 + z_m)^{-1/2}$ where z_m is the cosmological redshift of the mass. The density contrast is $\Delta(u, \boldsymbol{x}) = m\bar{\rho}^{-1} a^{-3}(u)\, \delta^{(3)}(\boldsymbol{x} - \boldsymbol{y})$, corresponding to $p = 0$. Such a static case is intended as a toy model only and is not realistic over long times or large scales.

For analytic computation rewrite (13) with (10a) as

$$z = 2\frac{m}{a_0} \int_{-y_1}^{x_e - y_1} ds\, \frac{s}{(s^2 + b^2)^{3/2}} (1 - y_1 - s)^{-2}$$

$$\left[\mathrm{erfc}(E) + (2/\sqrt{\pi})Ee^{-E^2}\right], \qquad (14)$$

where the photon is emitted at $x_e = 1 - \eta_e = 1 - (1 + z_e)^{-1/2}$, $y_1 = y \cos\theta$, $s = x - y_1$, and $s = 0$ corresponds to closest approach at impact parameter $b = y \sin\theta$. We have suppressed the subscript 0 on E. First consider the Newtonian case, where the bracketed quantity is unity. Around $s = 0$ the integrand is nearly odd so the dominant term from the symmetric part of the interval requires expanding $(1 - y_1 - s)^{-2}$ to obtain an overall term even in s. One readily sees that this gives a logarithmic integral $\sim \ln b^{-1}$. (Although the mass is static, the background is not so an energy shift is expected; but see the next subsection for the $p = 1$ case.)

Another interval giving a potentially large contribution is when $s \approx x_e - y_1$ or $x \approx x_e$. Here the integral varies as $(1 - x_e)^{-1} = (1 + z_e)^{1/2}$. Physically this corresponds to the early epoch when the universe was smaller and so the mass was nearer the source, or equivalently the mass per physical volume was greater. The final order of magnitude estimate is therefore $z \approx (m/a_0)[(1 + z_e)^{1/2} + \ln b^{-1}]$. For small angles $b \approx y\theta$. In terms of our original parametrization $m/a_0 \sim \epsilon^2 \kappa$ and $\theta \geq \kappa$ so the "Newtonian" result is $z_N \leq \epsilon^2 \kappa[(1 + z_e)^{1/2} + \ln \kappa^{-1}]$. Recall that $m/a_0 \approx 10^{-8}(m/10^{15}M_\odot)$, $10'' \approx 5 \times 10^{-5}$ radians so $\ln \kappa^{-1} \approx 10$, and the microwave background, for example, originates from $z_e \approx 10^3$ so $z_N = \mathcal{O}(100\, mH_0 < 10^{-6})$.

In the post-Newtonian case, near the mass the integrand is approximately the same, the correction factor being $1 + \mathcal{O}(E^3) \approx 1 + \mathcal{O}(\theta^3)$, while far away the Green function cuts off the contribution exponentially so $z_{PN} \sim mH_0 \ln \theta^{-1}$ only. The top half of Table 1 gives z in units of mH_0 for the static case, showing that the analytic dependences hold well.

4.1. Time varying point mass

We now examine $m = m_0(a/a_0)^p$, corresponding to an accreting (or evanescing) mass. In density perturbation theory inhomogeneities grow due to gravitational instability as a^1 in a $k = 0$

dust background. Here of course we are not restricted to linear fluctuations $\Delta \ll 1$; the parametrization, as can be seen from (2) or as discussed in JLW2, is $\mathcal{O}(\Delta) = \epsilon^2/\kappa^2$, which can be large.

The analog of (14) in the Newtonian limit is

$$z_N = 2\frac{m}{a_0} \int_{-y_1}^{x_e - y_1} ds \, \frac{s}{(s^2 + b^2)^{3/2}} (1 - y_1 - s)^{2(p-1)}. \qquad (15)$$

Again splitting up the interval we find near $s = 0$ that $z_N \approx (1 - p)(m/a_0) \ln b^{-1}$. As before, the other possibly significant contribution arises near $x = x_e$ (for $p < 1/2$) and is found to vary as $(1 - x_e)^{2p-1} = (1 + z_e)^{(1-2p)/2}$. Thus the total is $z_N \approx mH_0[(1 - p) \ln \theta^{-1} + (1 + z_e)^{(1-2p)/2}]$. This of course agrees when $p = 0$ with the static result, since $\theta \sim b \sim \kappa$. Inclusion of the post-Newtonian correction again cuts out the $1 + z_e$ contribution.

Note that for $p > 1/2$ the logarithm dominates. Also note that for $p = 1$, as in linear theory, we find $z_N = 2(m/a_0)[(s_o^2 + b^2)^{-1/2} - (s_e^2 + b^2)^{-1/2}]$ so if $s_o = -s_e$, i.e. the observer and emitter are situated symmetrically with respect to the inhomogeneity and so at the same value of gravitational potential, then there is zero redshift. Classically this corresponds to a ball gaining kinetic energy as it rolls into a dip then losing it coming out. If it rises to the same height on the far side and if the dip is time independent then its final velocity equals its initial. We see that for $p = 1$ the Newtonian potential is time independent and only the endpoints contribute – the usual result.

However, even for $p = 1$ and symmetric observer-emitter geometry there is a redshift (actually a blueshift) in the post-Newtonian case due to symmetry breaking by the distance dependence of the correction, i.e. roughly $\phi \sim a^0 \text{erfc}(E_0)$ which is neither symmetric nor time independent. The shift is of order mH_0, just as for the asymmetric endpoint case. The Sachs-Wolfe effect for point masses varying with time as a is given in the bottom half of Table 1. Because of the vanishing of the logarithmic term the results are angle independent (for small angles). For $p > 1$ the logarithmic term reappears and the results regain the angle dependence of the $p = 0$ case. The generalization to an extended matter distribution, e.g. a spherical density inhomogeneity, does not significantly affect the results (Kendall 1993).

The time dependent effect for a dynamically evolving isolated Newtonian density fluctuation, e.g. a cluster decoupled from the universal expansion, is sometimes known as the Rees-Sciama effect (Rees and Sciama 1968). A gravitational dynamical time scale is $(\bar{\rho}\Delta)^{-1/2} \sim \kappa/\epsilon$ so we expect $z \sim \int d\eta \, \partial_t \phi \sim b(\bar{\rho}\Delta)^{1/2}\phi$, parametrized as $\kappa \cdot \epsilon/\kappa \cdot \epsilon^2 \sim \epsilon^3$. Alternately consider an effective mass within a fixed comoving radius at the times a light ray enters and leaves the potential well: $m(t_{out}) \approx m(t_{in})[1 + \mathcal{O}(v/c)]$ with v the typical matter velocity, due to infall or peculiar motions. With an impulse approximation (15) becomes $z \sim mH_0 b^{-1} v \sim \epsilon^3$ since $v \sim \phi^{1/2} \sim \epsilon$ for bound systems. From this order of magnitude parametrization it is clear that to obtain a frequency shift (or equivalently temperature shift in the CMB) large enough to be observable

(say $> 10^{-6}$) one needs a rapid variation in the potential, more rapid than the gravitational time scale, such as from relativistic cosmic strings or black holes (but recall that the metric (1) was derived for nonrelativistic, weak field perturbations). Thus, within the context of a dynamical Sachs-Wolfe effect, the post-Newtonian formalism provides a significant but unobservable difference.

4.2. Fourier decomposition

For a more diffuse density distribution, e.g. a linear density field, it is convenient to Fourier decompose the gravitational potential into modes corresponding to a characteristic fluctuation wavelength, or density inhomogeneity length or mass scale. In fact, working in Fourier space allows simplification of many expressions. For example, to obtain the Laplacian $\nabla^2 \phi$ for arbitrary p, just transform (3), multiply by q^2, and perform the inverse transform. One finds that for general p, (11) is altered by a term $(a/a_0)^p$ multiplying $f(\boldsymbol{x})$ and a sum inside the integral of polynomials up to order p involving $|\boldsymbol{x} - \boldsymbol{y}|^2$ and C_0, multiplying the exponential.

Having seen that the variation of the gravitational potential over the photon propagation gives an insufficiently large effect to be readily observable, we are led to consider the effect of the potential at the endpoints of the path, i.e. at emitter and observer, on the photon energy. This gravitational redshift is simply $z = \phi_e - \phi_o$. Whereas in the isolated mass cases of Sect. 3.1, 3.2 we could ignore the initial condition term in (3), either by saying it provided a term in the redshift that just added independently to the propagation effect, or by realizing that its contribution was exponentially suppressed far from the mass, now when dealing with a density field and an endpoint effect we must treat it more carefully. Either we can ignore it by pushing $\eta_0 \to 0$, or include it in the calculation. We choose the latter.

We concentrate on the last scattering surface of the microwave background radiation and the density perturbations Δ_k there, writing the wavenumber from now on as k instead of q to agree with the usual notation in the literature. In the linear density perturbation regime Δ grows linearly with scale factor a, corresponding to our case $p = 1$. The mean square gravitational redshift is proportional to the sum over Fourier modes of the square of the gravitational potential, assuming random phases between modes: $\langle z^2 \rangle \sim \int d^3k \, |\phi_k|^2$. The magnitude of the temperature anisotropies $(\Delta T/T)^2 = \langle z^2 \rangle$ is usually characterized by the zero separation correlation function $C(0)$ but our case is slightly different. For lines of sight separated by some large angle ψ the two point correlation function $C(\psi) = \langle z(\boldsymbol{0}) \, z(\boldsymbol{\psi}) \rangle$ does not vanish because of the coherence introduced by the $\langle \phi_o^2 \rangle$ term. Rather than have $(\Delta T/T)^2 = 2[C(0) - C(\psi)] \to 2C(0)$ for ψ large, one has $(\Delta T/T)^2 \to \langle \phi_e^2 \rangle$, i.e. $\langle \phi_e^2 \rangle$ plays the role of the zero lag correlation in setting the magnitude. Alternately one can say that ϕ_o offers only a constant, isotropic shift so one can ignore it and consider only $z = \phi_e$.

This quantity can be written in terms of the density perturbation power spectrum by taking the Fourier transform of (8b),

but first we must evaluate the initial condition term of (3) and add it in. It is

$$\phi_k^{(ic)}(\eta) = [a(\eta_0)/a(\eta)]\,\phi_k(\eta_0)\,e^{-k^2 C_0}. \qquad (16)$$

Note the exponential suppression as η grows larger (later) than η_0. At this point we see that we really have two inputs to specify in (3), the initial density field $\Delta(\eta_0)$ and the initial potential $\phi(\eta_0)$. Because of the form of the full relativistic equation (2), both must be given. This is not unexpected though, because in JLW2 it was pointed out that (2) was essentially analogous to an inhomogeneous diffusion equation with time dependent parameters. It was found that the potential corresponded to the temperature in that sort of problem, and the density contrast to a heat source term. From that physical situation, however, we know that we must generally specify the initial distribution of both the temperature and the heat sources. It is only in the late time limit that the source completely determines the diffusive variable; in our case this corresponds (if compactness holds as well) to the Newtonian limit and the Poisson-Newton equation.

For the initial condition constant $\phi_k(\eta_0)$ we use the ansatz $\phi_k(\eta_0) = -4\pi A k^{-2} f_k$, so A gives the deviation from the Poisson equation ($A = 1$) in the initial conditions. Adding (16) to the transform of (8b) gives in terms of the density perturbation power spectrum

$$\langle z^2 \rangle = 16\pi^2 \int d^3k \, P_k k^{-4} \mathscr{C}_k,$$

$$\mathscr{C}_k =$$

$$\left[1 - (1-A)(\eta_0/\eta)^2 e^{-k^2 C_0} - 12 k^{-2} \eta^{-2}(1 - e^{-k^2 C_0})\right]^2, \quad (17)$$

where $P_k = |\Delta_k|^2$ is the density power spectrum and $C_0 = C(\eta_0, \eta)$ as given by (4).

Note that $\mathscr{C}$ gives the overall correction factor to the usual Poisson relation (in Fourier space) between the gravitational potential ϕ entering the metric (1) and the energy density; in particular, $\mathscr{C} = A^2$ at $\eta = \eta_0$. It can also be obtained directly from transforming the $p = 1$ version of the Laplacian (11). Thus $\mathscr{C}$ can be viewed alternately as giving the post-Newtonian adaptation of the endpoint Sachs-Wolfe effect, or as an effective alteration to the density power spectrum P_k, i.e. an effective transfer function. It is included in any (e.g. numerical) treatment using the full equation (2).

Depending on the initial conditions it has the possibility of either enhancing or suppressing the low Fourier modes, i.e. increasing or decreasing the large scale power in the intrinsic power spectrum P_k. This, for example, would cause a smaller (larger) overall normalization factor to be needed to match the large angle COBE microwave background anisotropy measurements, and hence also decrease (increase) the resultant predicted small scale power, thus ameliorating (exacerbating) the difficulties of the cold dark matter model.

The correction factor $\mathscr{C}_k$ is plotted in Fig. 1. In the late time limit, $\eta \gg \eta_0$, the results are independent of η/η_0 and A. From the expression in (17) or the figure, three regimes in
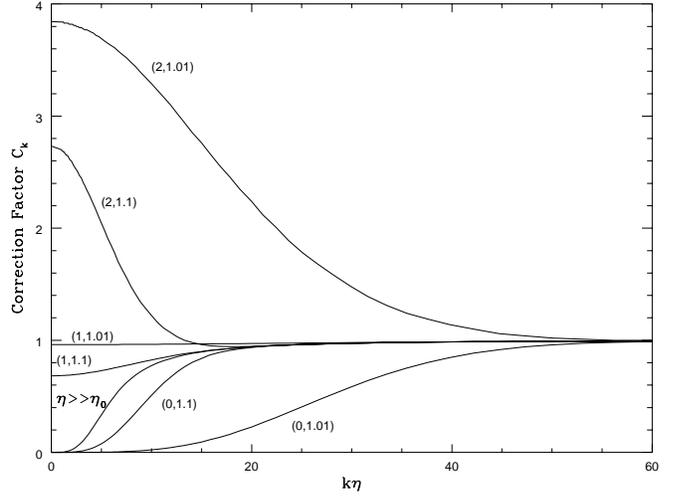

Fig. 1. The Poisson correction factor $\mathscr{C}_k = |\phi_k|^2/(16\pi^2 k^{-4} P_k)$ is plotted vs. $k\eta$ for various initial conditions $(A, \eta/\eta_0)$. For small wavenumbers (large scales) a significant enhancement or suppression can be achieved. The late time curve $\eta \gg \eta_0$ is independent of A.

perturbation wavelength can be identified. When $k \gg C_0^{-1/2}$, the factor is close to one, i.e. this is the late time, compact inhomogeneity Newtonian limit. For $\sqrt{12}\eta^{-1} \ll k \ll C_0^{-1/2}$, the factor begins to decline predominately due to the influence of the exponential, and when $k \ll \sqrt{12}\eta^{-1}$, the $(k\eta)^{-2}$ term becomes important as well, leading to $\mathscr{C}_k \to A^2(\eta_0/\eta)^4$. From Fig. 1, the deviation from the usual $P_k k^{-4}$ behavior of the Sachs-Wolfe effect becomes noticeable below $k\eta = 10-40$, depending on the value of C_0. Converting to wavelengths by

$$k\eta = 4\pi\eta/(H_0\lambda_0)$$

$$= 120\,(\lambda_0/10 h^{-1} Mpc)^{-1}[(1+z_e)/10^3]^{-1/2}, \qquad (18)$$

with λ_0 the present day wavelength and z_e the redshift of the last scattering surface, we see this corresponds to scales $\lambda_0 > 30 - 100\,h^{-1} Mpc$ or angular scales $\theta > (1/2) - 2°$, applicable to the COBE regime.

5. Conclusion

The pseudo-Newtonian gravitational potential appearing in the metric (1) that realistically approximates our universe, incorporating inhomogeneities in a FRW background, is related nontrivially to that density fluctuation distribution. The Green function (or kernel or propagator, in field theory terms) generally has a different spatial extent, or compactness, than the Newtonian case which corresponds to its late time, near neighborhood limit. In consequence, light propagation behavior for those regions of parameter space far from that limit differ from the Newtonian.

In the dynamical Sachs-Wolfe effect of the redshift induced by inhomogeneities along the light path, the deviation was shown to be significant but the overall magnitude too small to be observationally interesting. For the endpoint Sachs-Wolfe effect

of gravitational potential fluctuations at the source, the deviation could be viewed as an effective transfer function modifying the density perturbation power spectrum, with potentially important consequences for the normalization of the primordial density spectrum and hence the predictions of that model on smaller scales as a galaxy formation scenario.

References

Bardeen, J.M., 1980, PRD, 22, 1882

Futamase, T., 1989, MNRAS, 237, 187

Futamase, T., Schutz, B.F., PRD, 28, 2363

Jacobs, M.W., Linder, E.V., Wagoner, R.V., 1992, PRD, 45, R3292 (JLW1)

Jacobs, M.W., Linder, E.V., Wagoner, R.V., 1993, PRD, 48, 4623 (JLW2)

Kendall, J.S., 1993, unpublished MSc thesis, New Mexico State University

Kodama, H., Sasaki, M., 1984, Prog. Th. Phys. Supp, 78, 1

Ma, C-P., Bertschinger, E., 1995, ApJ, 455, 7

Rees, M.J., Sciama, D.W., 1968, Nat, 217, 511

Seljak, U., 1996, ApJ, 460, 549